Modulational instability in two-component discrete media with cubic-quintic nonlinearity

B. B. Baizakov,[1] A. Bouketir,[2] A. Messikh,[3] and B. A. Umarov[1,4]
[1]*Physical-Technical Institute, Uzbek Academy of Sciences, 100084 Tashkent, Uzbekistan*
[2]*Department of Mathematical Sciences, Community College, King Fahd University of Petroleum and Minerals, Dhahran 31261, Saudi Arabia*
[3]*Department of Science in Engineering, Faculty of Engineering, International Islamic University Malaysia, P.O. Box 10, 50728 Kuala Lumpur, Malaysia*
[4]*Department of Computational and Theoretical Sciences, Faculty of Science, International Islamic University Malaysia, P.O Box 141, 25710 Kuantan, Malaysia*

(Received 12 April 2008; revised manuscript received 4 January 2009; published 9 April 2009)

The effect of cubic-quintic nonlinearity and associated intercomponent couplings on the modulational instability (MI) of plane-wave solutions of the two-component discrete nonlinear Schrödinger (DNLS) equation is considered. Conditions for the onset of MI are revealed and the growth rate of small perturbations is analytically derived. For the same set of initial parameters as equal amplitudes of plane waves and intercomponent coupling coefficients, the effect of quintic nonlinearity on MI is found to be essentially stronger than the effect of cubic nonlinearity. Analytical predictions are supported by numerical simulations of the underlying coupled cubic-quintic DNLS equation. Relevance of obtained results to dense Bose-Einstein condensates (BECs) in deep optical lattices, when three-body processes are essential, is discussed. In particular, the phase separation under the effect of MI in a two-component repulsive BEC loaded in a deep optical lattice is predicted and found in numerical simulations. Bimodal light propagation in waveguide arrays fabricated from optical materials with non-Kerr nonlinearity is discussed as another possible physical realization for the considered model.

DOI: 10.1103/PhysRevE.79.046605 PACS number(s): 42.82.Et, 42.65.Sf, 03.75.Mn

I. INTRODUCTION

Modulational instability (MI) is a generic phenomenon in nonlinear physics responsible for spontaneous pattern formation both in uniform and nonuniform media. It occurs under combined effects of nonlinearity and dispersion (in temporal domain) or diffraction (in spatial domain), when the constant background wave becomes unstable against small amplitude periodic perturbations in a specific range of wave numbers [1]. MI is considered as a precursor to formation of localized nonlinear excitations, or soliton trains, and deeply studied since its recognition in the 1960s, in nonlinear optics [2], plasma physics [3], hydrodynamics [4], electrical transmission lines [5], and more recently in Bose-Einstein condensates (BECs) [6]. For comprehensive reviews of MI in Hamiltonian systems, both in continuous and discrete settings, the reader is addressed to Refs. [7–11].

Although the MI was originally predicted and explored for uniform media, later the phenomenon was experimentally observed in nonuniform media too, such as optical waveguide arrays [12], BEC in optical lattices [13], and layered Kerr media [14]. In Ref. [14] a quantitative agreement between theory, numerical simulations, and experiment on MI was found.

In a single-component system the effect of self-interactions is crucially important for the onset of MI. Among different soliton bearing wave equations, MI is most extensively studied, perhaps, in the context of continuous nonlinear Schrödinger equation, where the dispersion (diffraction) is always positive (excluding the situation of negative effective mass of BEC in optical lattices), so that MI occurs only with self-focusing nonlinearity. The condition for the MI is essentially modified for the discrete settings [15]. A unique feature of discrete optical waveguide arrays is that the diffraction can be either positive or negative, depending on the excitation angle, so that MI occurs with nonlinearity of either sign. Recently novel conditions for the onset of MI in a single-component DNLS equation with cubic-quintic nonlinearity were found in [16] and [17]. The authors have shown that the regions of self-trapping and stability of discrete breathers are drastically modified by the quintic nonlinear term, responsible for three-body effects in BEC. The effect of the trap potential on the MI of a single-component BEC with two- and three-body atomic interactions has been studied in a recent paper [18].

In multicomponent systems additional interaction mechanisms can arise that strongly affect the MI. A well-known example is the MI induced by a cross-phase modulation (XPM) in optical fibers in the normal group-velocity dispersion regime [19]. In this regime the nonlinearity-induced self-phase modulation (SPM) does not lead to MI of continuous waves in the scalar limit, while the MI and soliton formation are possible due to interaction between the two copropagating optical fields. MI in two-component BECs was addressed for the first time in [20]. In subsequent works [21] the MI and soliton formation in two-component BECs were investigated in details.

Among different possible scenarios of MI the most interesting one corresponds to the situation when both components are stable in the scalar limit, but unstable in presence of coupling between the components. This regime is especially relevant to BEC applications since only the condensates with repulsive interatomic forces are energetically and dynamically stable. In fact the stability of repulsive BEC allows to prepare the initial mixture of two noninteracting condensates and then switch on the interaction between the two components, for instance by a Feshbach resonance technique, to

study further evolution. Besides, glasses and organic materials, which are of significant interest for nonlinear optics [22–24], exhibit self-defocusing quintic nonlinearity in addition to focusing cubic one. Recently an optical cubic-quintic nonlinearity was observed in a colloid material [25], where the quintic nonlinearity may have both positive and negative signs. Bimodal light propagation at normal group-velocity dispersion in these materials corresponds to the above mentioned situation.

This work is aimed at studying the MI in a two-component DNLS equation that may arise due to the effect of cubic-quintic nonlinearity and associated intercomponent couplings. Of particular interest is the phase separation in a two-component BEC resulting from the MI, which was experimentally observed in [26]. The interpretation of this phenomenon based on the numerical integration of two coupled Gross-Pitaevskii equations with cubic nonlinearity was given in [27], where the underlying mechanism of the domain formation is found to be the MI induced by cross-phase modulation, which occurs in condensates with repulsive nonlinearity.

The present study of the MI in systems governed by coupled DNLS equations distinguishes itself from recent work on this topic in several ways. First, we address the effect of quintic nonlinearity on the MI and find it to be essentially stronger than the cubic nonlinearity in specific conditions. Second, combined effect of these two types of nonlinearities may induce the MI in those regions of the parameter space, where their individual action does not lead to MI. Finally, we reveal features of the phase separation of two-component BECs in deep optical lattices which result from the MI.

There are numerous potential physical realizations for the coupled DNLS equation considered in this work. For instance, mixtures of BECs (two distinct atomic species or two hyperfine states of the same atom) in deep optical lattices, when three-body effects [28] are essential, can be described by the coupled DNLS equation with cubic-quintic nonlinearity. It is appropriate to mention, however, that three-body effects are usually associated with an aspect limiting the lifetime of the condensate, which implies the existence of a nonzero imaginary part of the corresponding interaction term. Recently a regime has become experimentally attainable and a large BEC (containing $\sim 10^8$ sodium atoms) with a lifetime more than 3 s was created by suppressing three-body losses [29]. According to the estimate in Ref. [30]. the ratio between imaginary and real parts of the three-body interaction term for ^{87}Rb can be as small as $10^{-3}-10^{-4}$. A technique for strong suppression of three-body recombination in BECs using the resonant 2π laser pulses was developed in [31], where it was shown that reducing the decay rate of a BEC by several orders of magnitude is possible under realistic experimental conditions. This method is useful for extending the lifetime of condensates in the high-density regime and under the Feshbach resonance management. In these conditions our conservative model is valid. In general, the effect of three-body interactions in BECs can be either attractive or repulsive (corresponding to positive or negative quintic nonlinear term) and much stronger than two-body interactions [17].

In nonlinear optics, some materials with large nonlinear coefficients, such as chalcogenide glasses [22], colloids [25], and some organic polymers [23], also exhibit sufficiently high quintic nonlinearity at moderate optical wave intensity. In particular, polydiacetylene para-toluene sulfonate has one of the largest cubic nonlinearities known to date, also exhibits a significant negative quintic nonlinearity [24]. Note that although these materials possess a nonlinear loss, the characteristic soliton period can be made essentially smaller than the absorption length, so that the conservative model is justified. An appropriate mathematical framework for bimodal light propagation in waveguide arrays fabricated from such materials is the coupled DNLS equation with cubic-quintic nonlinearity. Also, the model considered here is relevant to bimodal light dynamics in media with saturable nonlinearity in the small amplitude limit, when the cubic-quintic nonlinearity can result from the expansion in series of the saturable nonlinearity. The phenomenon of discrete modulational instability in one-dimensional lattices with intensity-resonant nonlinearity has been considered in [32]. A general survey of the physics and mathematical tools for solitons in non-Kerr law optical media is given in the recent book [33].

The paper is structured as follows. In Sec. II the basic two-component DNLS equation is formulated, and the condition for the onset of MI is analytically derived from the linear stability analysis. Section III is devoted to numerical simulation of the evolution of perturbed plane-wave solutions to the coupled DNLS equation, and verification of the existence of MI in specific regions of the parameter space, according to prediction of the linear stability theory. In Sec. IV we analyze the phase separation in a two-component discrete system subject to MI. Finally, in Sec. V we summarize our findings.

II. MODEL AND CONDITIONS FOR MODULATIONAL INSTABILITY

The coupled DNLS equation with cubic-quintic nonlinearity, which is our basic model, has the following form:

$$i\frac{da_n}{dz} + c_a(a_{n+1} + a_{n-1}) + \lambda(|a_n|^2 + \beta|b_n|^2)a_n + \gamma(|a_n|^4 + 2\alpha|a_n|^2|b_n|^2 + \alpha|b_n|^4)a_n = 0, \quad (1)$$

$$i\frac{db_n}{dz} + c_b(b_{n+1} + b_{n-1}) + \lambda(|b_n|^2 + \beta|a_n|^2)b_n + \gamma(|b_n|^4 + 2\alpha|b_n|^2|a_n|^2 + \alpha|a_n|^4)b_n = 0, \quad (2)$$

where $a_n(z)$ and $b_n(z)$ are the complex amplitudes of the electromagnetic fields in the nth channel, in the case of the waveguide array, or the mean-field wave function at the nth site, in the BEC system, c_a and c_b are the linear coupling constants between adjacent waveguides in optics applications, which depend on the distance between waveguides, and both positive and negative values are relevant to discrete diffraction. In BEC applications these parameters characterize the tunnel coupling of the condensate fragments trapped in adjacent lattice sites, and depend on the strength of the

optical lattice. The variable z denotes propagation coordinate in optics applications, and time in BEC applications. The real parameters β and α are the cubic and quintic intercomponent nonlinear coupling (XPM) coefficients, respectively. The self-interaction (SPM) coefficients are re-scaled to one. The coefficients λ and γ, which although can be re-scaled to one, are retained for convenience to explore the effects of only cubic ($\gamma=0$), only quintic ($\lambda=0$), or weighted contribution of these two nonlinear terms ($\gamma\neq 0$, $\lambda\neq 0$) to overall MI. In the limit $\gamma=0$ and $\beta=1/\lambda$ Eqs. (1) and (2) transform into the coupled DNLS system considered in [34]. For $\beta=\alpha=0$ Eqs. (1) and (2) become decoupled, and split into two scalar DNLS equations with cubic-quintic nonlinearity, recently studied in the context of MI [16,17]. The MI gain spectra and domains of instability in the parameter space found in this work reproduce the results of Refs. [16,17,34] in the corresponding limits. Coupled DNLS systems (1) and (2) was employed in [35] for investigation of interactions between optical solitons in bimodal cubic-quintic media.

Equations (1) and (2) can be derived from the following Hamiltonian, assuming infinite lattice, or periodic boundary conditions:

$$H = H_a + H_b + H_{int}, \tag{3}$$

through

$$i\frac{da_n}{dz} = -\frac{\delta H}{\delta a_n^*}, \quad i\frac{db_n}{dz} = -\frac{\delta H}{\delta b_n^*}, \tag{4}$$

where

$$H_a = \sum_n \left[c_a(a_n^* a_{n+1} + a_n a_{n+1}^*) + \frac{\lambda}{2}|a_n|^4 + \frac{\gamma}{3}|a_n|^6 \right], \tag{5}$$

$$H_b = \sum_n \left[c_b(b_n^* b_{n+1} + b_n b_{n+1}^*) + \frac{\lambda}{2}|b_n|^4 + \frac{\gamma}{3}|b_n|^6 \right], \tag{6}$$

$$H_{int} = \sum_n [\beta\lambda|a_n|^2|b_n|^2 + \alpha\gamma(|a_n|^4|b_n|^2 + |a_n|^2|b_n|^4)]. \tag{7}$$

Two conserved quantities of Eqs. (1) and (2) are the Hamiltonian H and the total excitation norm (or power in nonlinear optics applications) $N=\Sigma_n(|a_n|^2+|b_n|^2)$. In the case of BEC this quantity bears the meaning of a total number of atoms in the condensate.

We investigate the stability of stationary plane-wave solutions of Eqs. (1) and (2),

$$a_n = a\exp(i[q_a n + k_a z]), \quad b_n = b\exp(i[q_b n + k_b z]), \tag{8}$$

with respect to small modulations of the amplitude and phase. Using ansatz (8) we get the following nonlinear dispersion relations:

$$k_a = 2c_a\cos(q_a) + \lambda(a^2 + \beta b^2) + \gamma(a^4 + 2\alpha a^2 b^2 + \alpha b^4), \tag{9}$$

$$k_b = 2c_b\cos(q_b) + \lambda(b^2 + \beta a^2) + \gamma(b^4 + 2\alpha a^2 b^2 + \alpha a^4). \tag{10}$$

Then we impose a slight modulation on plane waves (8),

$$\bar{a}_n = (a + \xi_n)\exp(i[q_a n + k_a z]),$$

$$\bar{b}_n = (b + \zeta_n)\exp(i[q_b n + k_b z]), \tag{11}$$

with

$$\xi_n = u_1\exp[i(Qn + Kz)] + u_2\exp[-i(Qn + Kz)], \tag{12}$$

$$\zeta_n = v_1\exp[i(Qn + Kz)] + v_2\exp[-i(Qn + Kz)], \tag{13}$$

where Q is the perturbation wave number. By inserting Eq. (11) into Eqs. (1) and (2) and performing a linearization we end up with an eigenvalue problem for the perturbation wave vector K,

$$\det\begin{bmatrix} -K + f_+ & \Lambda_a a^2 & \Lambda ab & \Lambda ab \\ \Lambda_a a^2 & K + f_- & \Lambda ab & \Lambda ab \\ \Lambda ab & \Lambda ab & -K + g_+ & \Lambda_b b^2 \\ \Lambda ab & \Lambda ab & \Lambda_b b^2 & K + g_- \end{bmatrix} = 0, \tag{14}$$

where

$$f_\pm = 2c_a[\cos(q_a \pm Q) - \cos(q_a)] + \Lambda_a a^2, \tag{15}$$

$$g_\pm = 2c_b[\cos(q_b \pm Q) - \cos(q_b)] + \Lambda_b b^2, \tag{16}$$

$$\Lambda_a = \lambda + 2\gamma(\alpha b^2 + a^2), \tag{17}$$

$$\Lambda_b = \lambda + 2\gamma(\alpha a^2 + b^2), \tag{18}$$

$$\Lambda = \lambda\beta + 2\gamma\alpha(a^2 + b^2). \tag{19}$$

Eigenvalue problem (14) can be recast in a more compact form

$$K^4 + p_3 K^3 + p_2 K^2 + p_1 K + p_0 = 0, \tag{20}$$

where p_i are coefficients depending on the parameters a, b, q, q_a, q_b, c_a, c_b, and λ. Explicit form of p_i are presented below by introducing notations $f_p=f_+$, $f_m=f_-$, $g_p=g_+$, and $g_m=g_-$,

$$p_3 = g_m - g_p + f_m - f_p, \tag{21}$$

$$p_2 = (g_m - g_p)(f_m - f_p) + a^4\Lambda_a^2 + b^4\Lambda_b^2 - f_m f_p - g_m g_p, \tag{22}$$

$$p_1 = (g_m - g_p)(a^4\Lambda_a^2 - f_m f_p) + (f_m - f_p)(b^4\Lambda_b^2 - g_p g_m), \tag{23}$$

$$\begin{aligned} p_0 = {} & [b^4(\Lambda_a\Lambda_b - 4\Lambda^2)\Lambda_a\Lambda_b + 2b^2(g_m + g_p)\Lambda^2\Lambda_a - g_m g_p\Lambda_a^2]a^4 \\ & + [2b^4(f_m + f_p)\Lambda^2\Lambda_b - b^2(f_m + f_p)(g_m + g_p)\Lambda^2]a^2 \\ & + (g_m g_p - b^4\Lambda_b^2)f_m f_p. \end{aligned} \tag{24}$$

For unstaggered case (adjacent elements are in phase) $q_a=q_b=0$ and staggered case (adjacent elements are out of phase) $q_a=q_b=\pi$ we have $f_m=f_p=f$ and $g_m=g_p=g$. Then $p_3=p_1=0$, meantime for p_0 and p_2 we have

$$p_2 = a^4\Lambda_a^2 + b^4\Lambda_b^2 - f^2 - g^2, \tag{25}$$

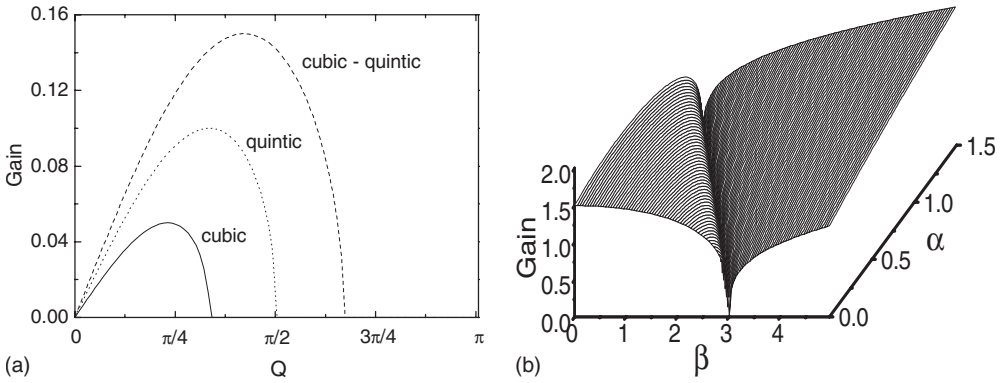

FIG. 1. (a) Gain spectra for the perturbation wave number in the interval $Q \in [0, \pi]$ according to Eq. (28) for the cases when only cubic ($\lambda=0.95$, $\gamma=0$, solid line), only quintic ($\lambda=0$, $\gamma=0.95$, dotted line), and cubic-quintic ($\lambda=\gamma=0.95$, dashed line) nonlinear terms are present in coupled system equations (1) and (2). Initial plane-wave amplitudes and coefficients of intercomponent coupling are $a=b=1$, $\beta=1/\lambda$, $\alpha=1/\gamma$, respectively. All curves pertain to the staggered mode with $c_a=c_b=-0.1$. (b) Gain of MI as a function of the cubic and quintic intercomponent coupling strengths β and α according to Eq. (28) for parameters $a=b=1$, $\lambda=\gamma=1$, $c_a=-0.1$, and $c_b=0.1$ (staggered and unstaggered modes in two components).

$$p_0 = [b^4(\Lambda_a\Lambda_b - 4\Lambda^2)\Lambda_a\Lambda_b + 4b^2g\Lambda^2\Lambda_a - g^2\Lambda_a^2]a^4 + 4b^2f\Lambda^2(b^2\Lambda_b - g)a^2 + (g^2 - b^4\Lambda_b^2)f^2. \quad (26)$$

It should be pointed out that changing from the above mentioned unstaggered configuration to the staggered one can entail sign changes in the first term in f and g. Since terms such as g_m+g_p and f_m+f_p occur linearly in p_0 of Eq. (24), these sign-changes crucially affect the MI [see Eq. (28) below]. In numerical simulations we consider both signs for the first term in f and g by giving appropriate signs to coefficients c_a and c_b in Eqs. (15) and (16). Specifically, we assume $c_{a,b}<0$ when considering staggered configuration, and $c_{a,b}>0$ for unstaggered case. Now the characteristic equation is reduced to following form:

$$K^4 + p_2K^2 + p_0 = 0. \quad (27)$$

The gain (growth rate) of modulational instability can be straightforwardly calculated from Eq. (27),

$$G = |\mathrm{Im}\ K| = \frac{1}{2^{1/2}}|\mathrm{Im}[-p_2 \pm \sqrt{p_2^2 - 4p_0}]^{1/2}|. \quad (28)$$

The MI of plane-wave solutions of Eqs. (1) and (2) in the case when only cubic nonlinearity is present was investigated in Ref. [34]. It can be easily verified that the MI gain spectra and domains of instability given by Eq. (28) reproduce the results of [34] at $\gamma=0$ and $\beta=1/\lambda$.

Simple analytic expressions for Eq. (28) can be obtained for particular sets of parameters. For instance, if in Eqs. (1) and (2) only cubic nonlinearity is present ($\gamma=0$, $\lambda\neq0$), and $a=b=1$, $c_a=c_b=c$, $\beta=1/\lambda$, we have $\Lambda_a=\Lambda_b=\lambda$ and $\Lambda=1$. Then we get the MI growth rate for the cubic nonlinearity

$$G_c = 2^{3/2}\left|\mathrm{Im}\left\{-c\ \sin^2\left(\frac{Q}{2}\right)\left[-2c\ \sin^2\left(\frac{Q}{2}\right) + \lambda \pm 1\right]\right\}^{1/2}\right|. \quad (29)$$

Similarly, when the only quintic nonlinearity is present ($\lambda=0$, $\gamma\neq0$) and $a=b=1$, $c_a=c_b=c$, $\alpha=1/\gamma$, we have $\Lambda_a=\Lambda_b=2(\gamma+1)$ and $\Lambda=4$, which yields the MI growth rate for the quintic nonlinearity,

$$G_q = 4\left|\mathrm{Im}\left\{-c\ \sin^2\left(\frac{Q}{2}\right)\left[-c\ \sin^2\left(\frac{Q}{2}\right) + (\gamma+1) \pm 2\right]\right\}^{1/2}\right|. \quad (30)$$

Finally, when both cubic and quintic nonlinearities are present ($\lambda\neq0$, $\gamma\neq0$) and $a=b=1$, $c_a=c_b=c$, $\beta=1/\lambda$, $\alpha=1/\gamma$, we have $\Lambda_a=\Lambda_b=\lambda+2(\gamma+1)$ and $\Lambda=5$, which yields

$$G_{cq} = 2^{3/2}\left|\mathrm{Im}\left\{-c\ \sin^2\left(\frac{Q}{2}\right)\left[-2c\ \sin^2\left(\frac{Q}{2}\right) + \lambda + 2(\gamma+1) \pm 5\right]\right\}^{1/2}\right|. \quad (31)$$

Since the growth rates of MI given by Eqs. (29)–(31) are even functions of the perturbation wave number Q, we restrict to consideration of only positive values of this parameter (for negative Q the curves are symmetric with respect to the Gain axis).

The onset of MI is defined from the condition that the expression under the square root in above equations acquires a negative value. For instance, the staggered mode ($c<0$) with cubic nonlinearity ($\lambda\neq0$, $\gamma=0$) is unstable when $|Q| < 2\arcsin[\sqrt{0.5(\lambda-1)/c}]$, while with quintic nonlinearity ($\lambda=0$, $\gamma\neq0$) it is unstable when $|Q|<2\arcsin[\sqrt{(\gamma-1)/c}]$. In the presence of both types of nonlinearities ($\gamma\neq0$, $\lambda\neq0$) the instability is observed when $|Q| < 2\arcsin[\sqrt{0.5(\lambda+2\gamma-3)/c}]$. Threshold perturbation wave numbers for the existence of MI at $\lambda=\gamma=0.95$ and $c=-0.1$, predicted by these formulas for the cases of cubic, quintic, and cubic-quintic nonlinearities are equal to $Q_c^{thr}=1.05$, $Q_q^{thr}=1.57$, and $Q_{cq}^{thr}=2.09$, respectively. Similarly, the values of perturbation wave numbers, corresponding to maximal growth rates of MI are determined from the extremum (first derivative with respect to Q is zero) of the expression under the square root in Eqs. (29)–(31) as $Q_c^{max}=0.72$, $Q_q^{max}=1.05$, and $Q_{cq}^{max}=1.32$. These analytical predictions corroborate

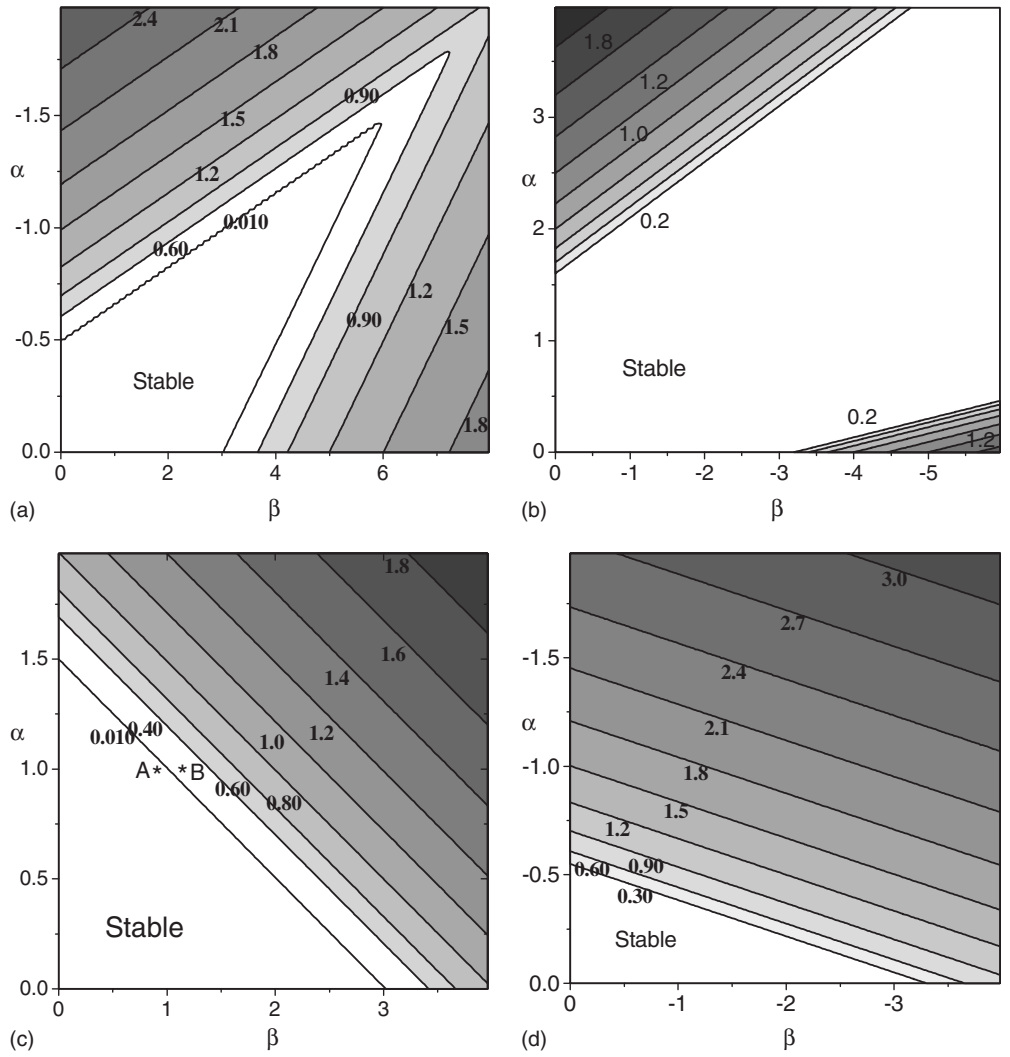

FIG. 2. Instability domains (shaded), corresponding to different signs of intercomponent interaction in Eqs. (1) and (2) for the parameter set $a=1.01$, $b=1.00$, $\lambda=\gamma=1$, and $c_a=c_b=-0.1$. Figures indicate the growth rate of instability (MI gain). (a) $\beta>0$, $\alpha<0$. (b) $\beta<0$, $\alpha>0$. (c) $\beta>0$, $\alpha>0$. (d) $\beta<0$, $\alpha<0$.

with numerical calculations using the general formula (28), as can be observed in Fig. 1(a).

To illustrate the role of specific nonlinearities and associated intercomponent couplings in modification of the MI conditions, we performed comparison between the cases of purely cubic, purely quintic, and cubic-quintic nonlinearity, as shown in Fig. 1. It is evident from Fig. 1(a) that for the same set of parameters the quintic nonlinearity leads to significant extension of the instability domain and greater value of the gain parameter, compared to contribution of the cubic nonlinearity, e.g., for $1.05<Q<\pi/2$. Moreover, combined effect of these two nonlinear terms gives rise to instability in regions of the parameter space, where their individual contributions are zero, e.g., at $Q\in[\pi/2,2.09]$. It should be also pointed out that the uncoupled system ($\alpha=\beta=0$) is modulationally stable for $c_a<0$, $c_b<0$, $\lambda>0$, and $\gamma>0$, which means that the instability is caused by intercomponent couplings (XPM). Nontrivial superposition of the cubic (β) and quintic (α) intercomponent couplings leads to suppression of the MI along the line $\beta+2\alpha=3$ for a given set of parameters, as illustrated in Fig. 1(b). In the context of BEC opposing signs of dispersion and diffraction and nonlinearity (e.g., negative c_a and c_b and positive nonlinear terms) corresponds to repulsive nonlinearity of both components, which is the most frequently encountered experimental setting with double-specie mixture condensates [36,37]. In further analysis more emphasis will be given to this particular case.

Domains of instability corresponding to maximum of MI gain in $Q\in[0,\pi]$ for different combination of parameters are shown in Figs. 2 and 3. With regard to the existing link between the phenomenon of MI and soliton formation in the system, an important conclusion can be drawn from these figures in the context of mixture BECs. Although the individual repulsive condensates in the absence of optical lattice do not support stable bright solitons, they can emerge due to the periodic potential of the deep optical lattice and intercomponent couplings in the mixture condensate. In particular, when both condensates are repulsive (see Fig. 2), a sufficiently strong intercomponent interaction of at least one of the two types, cubic (β), or quintic (α), induces MI, therefore generates discrete vectorial solitons.

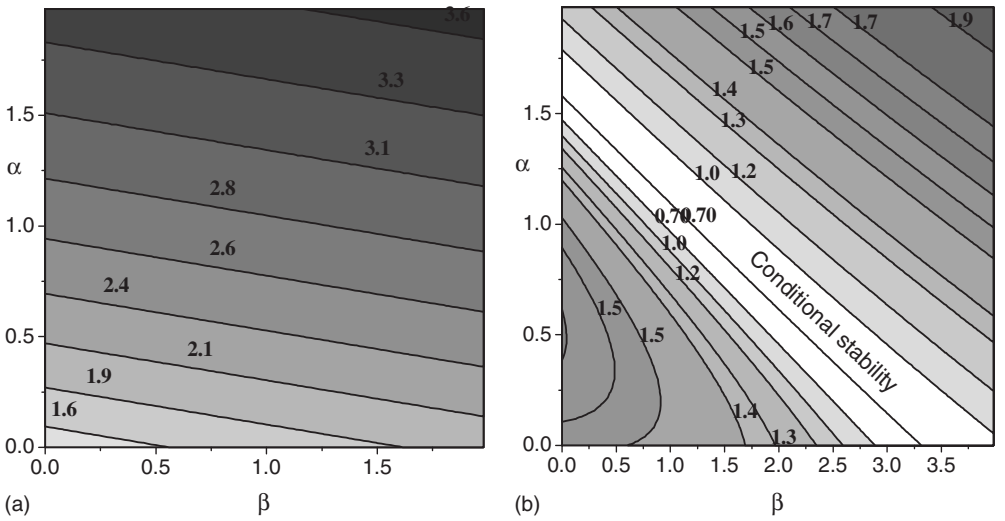

FIG. 3. Instability domains (shaded), corresponding to maximal gain in Eq. (28) as a function of the cubic and quintic intercomponent coupling coefficients in Eqs. (1) and (2) at parameters $a=b=1$, $\lambda=\gamma=1$, and $\alpha>0$, $\beta>0$. Figures indicate the growth rate of instability (MI gain). (a) All attractive case, $c_a=c_b=0.1$. (b) One component is attractive, the other is repulsive $c_a=0.1$, $c_b=-0.1$. The region of conditional stability corresponds to low MI growth rate.

On the other hand, the attractive intracomponent and intercomponent interactions are usually associated with the collapse instability of BECs [38]. In order to avoid the collapse, Bose condensation of atoms with a natural negative scattering length, like ^{7}Li, ^{85}Rb, is produced initially in a repulsive state using a Feshbach resonance technique, which allows to change the magnitude and sign of atomic interactions by means of external magnetic fields near particular resonances. That is why the existence of MI and soliton formation in the case of all repulsive interactions, i.e., when the condensate is stable against collapse, is especially interesting [see Fig. 2(c)]. In particular, symbiotic discrete solitons on a finite background can exist in this case [34]. This result contrasts with the two-component BEC in the continuous model without optical lattice because all repulsive interactions in that case gives rise to a phase separation with small spatial overlap of components [39].

The onset of MI is differently influenced by the cubic and quintic nonlinearities. The role of quintic nonlinearity and associated intercomponent couplings in this process appears to be stronger than the cubic one. This is evident from the fact that for the same set of parameter values, the coefficient of quintic intercomponent interaction can be two times weaker than the cubic one, in order to induce the MI for selected parameters, as shown in Fig. 2(c). In the case of all attractive interactions the system is always modulationally unstable [Fig. 3(a)]. In the meantime, if one of the components is attractive and the other is repulsive, conditions for the onset of MI is essentially different, as shown in Fig. 3(b). Stability domain shrinks into a narrow strip, where the MI

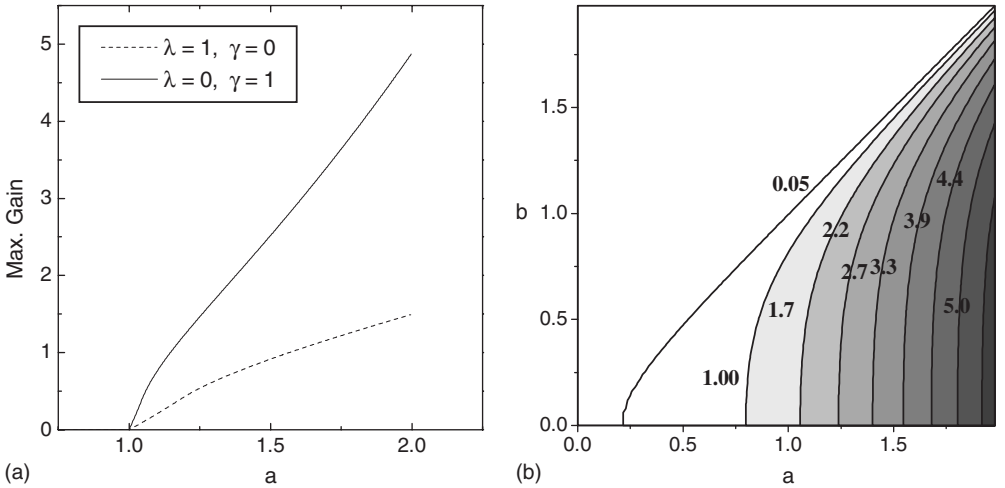

FIG. 4. (a) Contribution of only cubic (dashed line) and only quintic (solid line) nonlinearity to the MI at different amplitudes of the plane wave a at $b=1$ according to Eq. (28). (b) Regions of instability (shaded) in the plane (a,b) according to Eq. (28). Figures indicate the maximal growth rate of MI at given parameters. For both panels the parameter set corresponds to $c_a=0.1$, $c_b=-0.1$, $\lambda=\gamma=1$, and $\alpha=\beta=1$.

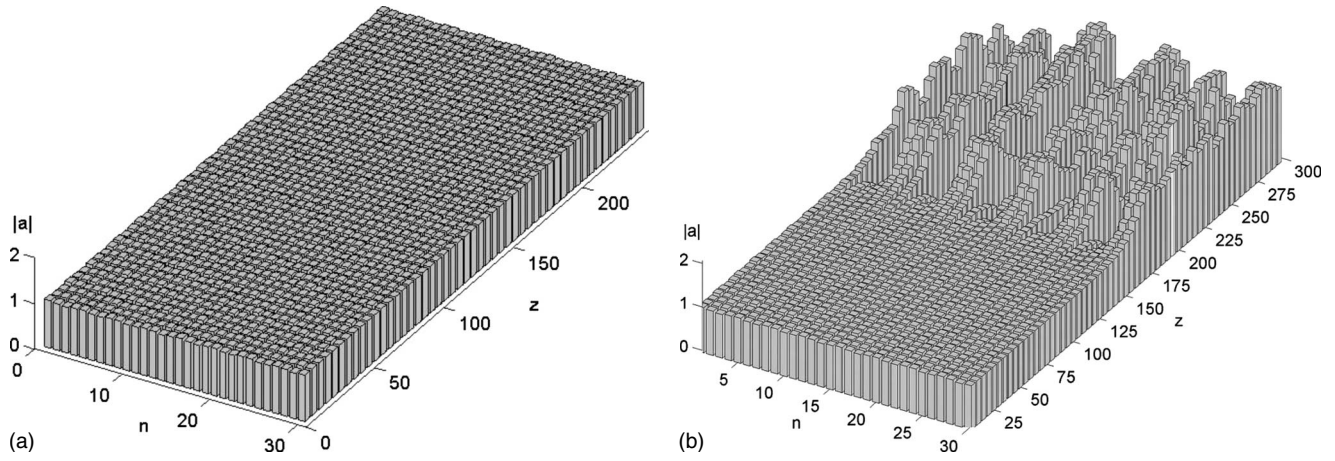

FIG. 5. Evolution of the weakly perturbed plane-wave solution $\bar{a}=a+\xi(n)$ with $\xi(n)=0.01\cos\{8\cdot 2\pi/N\cdot(n-1)\}$ governed by Eqs. (1) and (2) for $\lambda=\gamma=1$, $a=1.01$, $b=1.00$, $c_a=c_b=-0.1$, and two sets of intercomponent coupling coefficients. (a) The values $\alpha=1.0$ and $\beta=0.9$ correspond to point A in white area of Fig. 2(c), where the MI gain is negligible, and the wave propagation is stable. (b) MI develops for $\alpha=1.0$ and $\beta=1.1$, corresponding to point B in shaded area of Fig. 2(c), where MI gain is nonzero. The number of lattice sites is $N=30$. Evolution of the component $\bar{b}=b+\xi(n)$ is qualitatively similar to $\bar{a}$ and not shown here.

gain is very small, but finite. For selected parameters the MI gain equals to zero only along the straight-line connecting points $\alpha=1.5$ and $\beta=3.0$. This arrangement can be relevant to the recent experiment with a two-species BEC of ^{85}Rb and ^{87}Rb atoms [37]. In normal conditions ^{85}Rb BEC features attractive atomic interactions, while ^{87}Rb BEC is repulsive. Strength and sign of intercomponent interactions in this two-species BEC was shown to be tunable by a Feshbach resonance technique [37]. As said above, in experiments with BEC both the intra-atomic and interatomic scattering lengths can be varied by external magnetic or light fields. Therefore, it is pertinent to consider the MI for different values of coupling parameters α and β as shown in Figs. 2 and 3. Meanwhile, in nonlinear optics the relevant variables are the intensities (or amplitudes) of the light fields a and b. In Fig. 4 the maximum gain of MI is plotted as a function of the plane-wave amplitudes. The stronger effect of the quintic nonlinearity on MI compared to the cubic one is evident from Fig. 4(a) as the corresponding gain of MI increases more rapidly. Note the absence of instability when $a<1$. In Fig. 4(b) the instability domain is shown by shaded areas in the parameter space of plane-wave amplitudes $a-b$ when both the cubic and quintic nonlinearities contribute to the MI.

III. NUMERICAL SIMULATIONS OF MODULATIONAL INSTABILITY

The linear stability analysis allows to identify particular regions in the parameter space where MI may occur, and estimate the growth rate of perturbations according to Eq. (28). However, the linear stability theory does not predict further evolution of the wave field. To study the evolution of the wave field under MI and pattern formation in the system one has to recourse to numerical simulations of the governing DNLS (1) and (2).

Toward this objective we performed numerical simulations of basic DNLS systems (1) and (2) with a perturbed plane-wave initial conditions as per Eqs. (8), (12), and (13). Equations (1) and (2) represent a system of coupled ordinary differential equations (ODEs) for $2n$ complex variables a_n and b_n, where n is the number of lattice sites. To simulate the evolution of these variables in z we impose the periodic boundary conditions. For numerical integration of the ODE system we employ the fifth-order Runge-Kutta procedure with adaptive step-size control [40]. To ensure the accuracy of computations we monitor the conserved quantities of the problem, such as the norm (power in optics applications, and total number of atoms in the case of BEC) and Hamiltonian, to precision $\sim 10^{-6}$.

When the parameter set corresponds to white areas in Figs. 2 and 3 where the growth rate of instability (MI gain) is negligible, the plane-wave solutions remain unaltered while propagating along z [see Fig. 5(a)]. On the contrary, when the parameters correspond to dark areas in Figs. 2 and 3, the MI sets in giving rise to localized states, as illustrated in Fig. 5(b). We are reminded that the linear stability analysis provides only the condition for the onset of MI, but does not tell more about further evolution of the wave field. Long-term evolution of the wave pattern shown in Fig. 5 is beyond the linear theory.

IV. PHASE SEPARATION

Two component BECs have a tendency to separate into single-component domains in absence of external potentials [39]. Interparticle interactions between the different components control the miscibility of condensates. In the meantime, the strength of interaction between the components is critical for the possibility of MI in mixture BECs. The MI can be a precursor for the phase separation in multicomponent nonlinear media.

The periodic potential of the optical lattice modifies the conditions for the MI and suppresses phase separation [41]. When the optical lattice is sufficiently strong, the system is

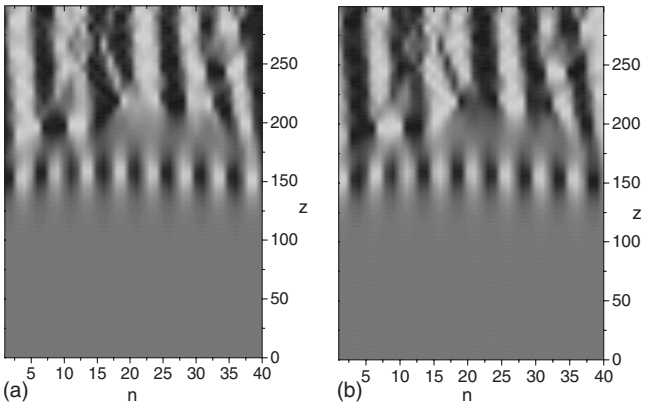

FIG. 6. The perturbed initial plane-wave solution $a+\xi(n)$ and $b+\xi(n)$ with $\xi_n=0.01\cos(2\pi mn/40)$, $m=8$ develops instability and breaks into localized states at $z\simeq 150$ when the parameter set corresponds to point B in shaded area of Fig. 2(c) with nonzero MI gain: $a=1.01$, $b=1.00$, $c_a=c_b=-0.1$, $\alpha=1.0$, $\beta=1.1$, and $\lambda=\gamma=1$. Density is represented by intensity of shading. Darker areas correspond to higher amplitudes of the wave. Formation of domains entirely consisting of components (a) and (b) is indication of the phase separation.

modeled by discrete NLS equations (1) and (2). In these conditions the phase separation can show up as periodically arranged domains of single components emerged from the initially homogeneous mixture. Figure 6 illustrates this phenomenon through the density plots of components (a) and (b) for the case when both the intracomponent and intercomponent interactions in BEC are repulsive. Similar numerical experiment when the evolution takes place under the effect of only quintic nonlinearity is shown in Fig. 7. Although spatially periodic structure consisting of single phases emerge due to the MI at $z\simeq 150$ in Fig. 6 and at $z\simeq 100$ in Fig. 7, further evolution breaks the spatial order. Recurrence into homogeneously mixed initial state does not happen, whereas the phase separation persists.

One of the powerful tools for manipulation of atomic interactions in BECs is provided by the Feshbach resonance phenomenon [42]. Tunability of both intracomponent and intercomponent two-body atomic scattering lengths by the Feshbach resonance technique makes it relevant to consider the situation, when the cubic nonlinearity and associated coupling parameter are set to zero from the beginning (see Fig. 7), or when the phase separation occurred. Numerical simulation of this situation is shown in Fig. 8 for the all repulsive case with parameters corresponding to point B in Fig. 2(c). Redistribution of the phases can be suppressed also by increasing the strength of the optical lattice, when localized structures are formed. Since the coefficients c_a and c_b, which are proportional to the probability of atom tunneling between adjacent lattice cites and depend on the strength of the optical lattice, this can be modeled by instantly decreasing the values of c_a and c_b when the phase separation occurred.

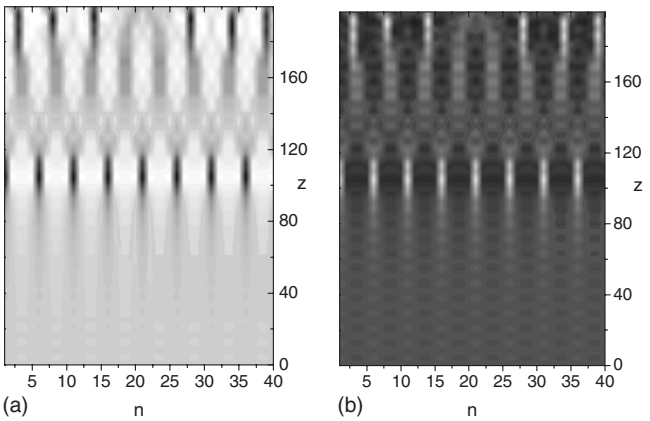

FIG. 7. Phase separation under the effect of only quintic nonlinearity and associated intercomponent couplings according to numerical simulation of Eqs. (1) and (2) for parameters $a=0.5$, $b=1.0$, $c_a=0.1$, $c_b=-0.1$, $\alpha=\beta=0.9$, $\lambda=0$, and $\gamma=1.0$.

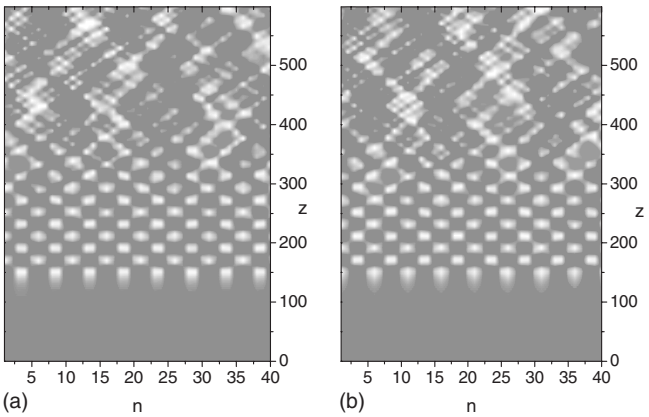

FIG. 8. Phase separation due to MI in all repulsive case, when the cubic nonlinearity and associated intercomponent coupling in Eqs. (1) and (2) are set to zero ($\lambda=0$) at $z=150$. Further evolution takes place under the effect of only quintic nonlinearity. Parameters are the same as in Fig. 6. Few periodic oscillations of the spatial arrangement of phases (a) and (b) is observed, before irregular distribution of phases sets in.

V. CONCLUSIONS

We have studied conditions for the onset of modulational instability in a two-component system described by coupled discrete nonlinear Schrödinger equations with cubic-quintic nonlinearity. The proposed model can be applied to mixtures of Bose-Einstein condensates loaded in deep optical lattices when three-body effects are essential, and bimodal light propagation in optical waveguide arrays made of materials featuring significant quintic nonlinearity. Analytical expression for the MI gain spectra is obtained and the regions of instability of plane-wave solutions in the parameter space of the governing coupled DNLS are identified. For the similar initial conditions such as equal amplitudes of plane waves and equal strengths of intercomponent couplings, the effect of quintic nonlinearity on the MI is found to be stronger compared to the effect of cubic nonlinearity. In some regions of the parameter space combined action of the cubic-quintic nonlinearity can induce the modulational instability, whereas individual action of the cubic or quintic nonlinearity does not lead to instability. By means of numerical simulations we

explored phase separation in a two-component discrete medium induced by modulational instability. Spatially periodic structure of alternating phases emerged at initial stage of the evolution later transforms into irregular pattern. If the cubic nonlinearity is set to zero at particular instance of the evolution, the periodic pattern formation is observed.

ACKNOWLEDGMENTS

This work has been supported by the Ministry of Higher Education, Malaysia under research Grant No. IIUM/504/RES/G/14/11/02/FRGS0106-29. B.B.B. is grateful to the Department of Science in Engineering, IIUM, Malaysia, for their hospitality.

[1] *Encyclopedia of Nonlinear Science*, edited by A. Scott (Routledge, New York, 2005).

[2] V. I. Bespalov and V. I. Talanov, Zh. Eksp. Teor. Fiz., Pis'ma Red. **3**, 471 (1966) [JETP Lett. **3**, 307 (1966)]; L. A. Ostrovskii, Zh. Eksp. Teor. Fiz. **51**, 1189 (1966) [Sov. Phys. JETP **24**, 797 (1967)]; V. I. Karpman, Zh. Eksp. Teor. Fiz., Pis'ma Red. **6**, 829 (1967) [JETP Lett. **6**, 277 (1967)].

[3] G. A. Askar'yan, Zh. Eksp. Teor. Fiz. **42**, 1567 (1962) [Sov. Phys. JETP **15**, 1088 (1962)]; Y. Taniuti and H. Washimi, Phys. Rev. Lett. **21**, 209 (1968); C. K. W. Tam, Phys. Fluids **12**, 1028 (1969); A. Hasegawa, Phys. Rev. Lett. **24**, 1165 (1970).

[4] G. B. Whitham, Proc. R. Soc. London, Ser. A **283**, 238 (1965); T. B. Benjamin and J. E. Feir, J. Fluid Mech. **27**, 417 (1967).

[5] P. Marquie, J. M. Bilbault, and M. Remoissenet, Phys. Rev. E **49**, 828 (1994); Fabien II Ndzana, Alidou Mohamadou, and Timoleon Crepin Kofane, J. Phys. D **40**, 3254 (2007).

[6] B. Wu and Q. Niu, Phys. Rev. A **64**, 061603(R) (2001); V. V. Konotop and M. Salerno, *ibid.* **65**, 021602(R) (2002); B. B. Baizakov, V. V. Konotop, and M. Salerno, J. Phys. B **35**, 5105 (2002); A. Smerzi, A. Trombettoni, P. G. Kevrekidis, and A. R. Bishop, Phys. Rev. Lett. **89**, 170402 (2002); Z. Rapti, P. G. Kevrekidis, A. Smerzi, and A. R. Bishop, J. Phys. B **37**, S257 (2004); P. G. Kevrekidis and D. J. Frantzeskakis, Mod. Phys. Lett. B **18**, 173 (2004).

[7] E. A. Kuznetsov, A. M. Rubenchik, and V. E. Zakharov, Phys. Rep. **142**, 103 (1986).

[8] A. Hasegawa and Y. Kodama, *Solitons in Optical Communications* (Clarendon, Oxford, 1995).

[9] N. N. Akhmediev and A. Ankievich, *Solitons: Nonlinear Pulses and Beams* (Chapman and Hall, London, 1997).

[10] F. Kh. Abdullaev, S. A. Darmanyan, and J. Garnier, in Progress in Optics, Vol. 44, edited by E. Wolf (Elsevier, Amsterdam, 2002), p. 303.

[11] F. Lederer, G. I. Stegeman, D. N. Christodoulides, G. Assanto, M. Segev, and Y. Silberberg, Phys. Rep. **463**, 1 (2008).

[12] J. Meier, G. I. Stegeman, D. N. Christodoulides, Y. Silberberg, R. Morandotti, H. Yang, G. Salamo, M. Sorel, and J. S. Aitchison, Phys. Rev. Lett. **92**, 163902 (2004).

[13] F. S. Cataliotti, L. Fallani, F. Ferlaino, C. Fort, P. Maddaloni, and M. Inguscio, New J. Phys. **5**, 71 (2003).

[14] M. Centurion, M. A. Porter, Y. Pu, P. G. Kevrekidis, D. J. Frantzeskakis, and D. Psaltis, Phys. Rev. Lett. **97**, 234101 (2006).

[15] Yu. S. Kivshar and M. Peyrard, Phys. Rev. A **46**, 3198 (1992).

[16] F. Kh. Abdullaev, A. Bouketir, A. Messikh, and B. A. Umarov, Physica D **232**, 54 (2007).

[17] Ai-Xia Zhang and Ju-Kui Xue, Phys. Lett. A **372**, 1147 (2008).

[18] Etienne Wamba, Alidou Mohamadou, and Timoleon C. Kofane, Phys. Rev. E **77**, 046216 (2008).

[19] G. P. Agrawal, Phys. Rev. Lett. **59**, 880 (1987).

[20] E. V. Goldstein and P. Meystre, Phys. Rev. A **55**, 2935 (1997).

[21] N. A. Kostov, V. Z. Enolskii, V. S. Gerdjikov, V. V. Konotop, and M. Salerno, Phys. Rev. E **70**, 056617 (2004); Guang-Ri Jin, Chul Koo Kim, and Kyun Nahm, Phys. Rev. A **72**, 045601 (2005); K. Kasamatsu and M. Tsubota, *ibid.* **74**, 013617 (2006); J. Ruostekoski and Z. Dutton, *ibid.* **76**, 063607 (2007).

[22] F. Smektala, C. Quemard, V. Couderc, and A. Barthelemy, J. Non-Cryst. Solids **274**, 232 (2000); G. Boudebs, S. Cherukulappurath, H. Leblond, J. Troles, F. Smektala, and F. Sanchez, Opt. Commun. **219**, 427 (2003).

[23] C. Zhan, D. Zhang, D. Zhu, D. Wang, Y. Li, D. Li, Z. Lu, L. Zhao, and Y. Nie, J. Opt. Soc. Am. B **19**, 369 (2002).

[24] B. Lawrence, W. E. Torruellas, M. Cha, M. L. Sundheimer, G. I. Stegeman, J. Meth, S. Etemad, and G. Baker, Phys. Rev. Lett. **73**, 597 (1994).

[25] E. L. Falcao-Filho, C. B. de Araujo, and J. J. Rodrigues, Jr., J. Opt. Soc. Am. B **24**, 2948 (2007).

[26] H.-J. Miesner, D. M. Stamper-Kurn, J. Stenger, S. Inouye, A. P. Chikkatur and W. Ketterle, Phys. Rev. Lett. **82**, 2228 (1999).

[27] K. Kasamatsu and M. Tsubota, Phys. Rev. Lett. **93**, 100402 (2004).

[28] F. Kh. Abdullaev, A. Gammal, Lauro Tomio, and T. Frederico, Phys. Rev. A **63**, 043604 (2001); E. Braaten and H.-W. Hammer, Phys. Rev. Lett. **87**, 160407 (2001); T. Kohler, *ibid.* **89**, 210404 (2002); W. P. Zhang, E. M. Wright, H. Pu, and P. Meystre, Phys. Rev. A **68**, 023605 (2003); F. Kh. Abdullaev and M. Salerno, *ibid.* **72**, 033617 (2005).

[29] K. M. R. van der Stam, R. Meppelink, J. M. Vogels, and P. van der Straten, Phys. Rev. A **75**, 031602(R) (2007).

[30] Ai-Xia Zhang and Ju-Kui Xue, Phys. Rev. A **75**, 013624 (2007).

[31] Chris P. Search, Weiping Zhang, and Pierre Meystre, Phys. Rev. Lett. **92**, 140401 (2004).

[32] M. Stepic, A. Maluckov, M. Stojanovic, F. Chen, and D. Kip, Phys. Rev. A **78**, 043819 (2008).

[33] Anjan Biswas and Swapan Konar, *Introduction to Non-Kerr Law Optical Solitons* (Chapman & Hall, London, 2006).

[34] A. Kobyakov, S. Darmanyan, F. Lederer, and E. Schmidt, Opt. Quantum Electron. **30**, 795 (1998).

[35] A. Maimistov, B. Malomed, and A. Desyatnikov, Phys. Lett. A **254**, 179 (1999); A. S. Desyatnikov, D. Mihalache, D. Mazilu, B. A. Malomed, C. Denz, and F. Lederer, Phys. Rev. E **71**, 026615 (2005).

[36] G. Modugno, M. Modugno, F. Riboli, G. Roati, and M. Inguscio, Phys. Rev. Lett. **89**, 190404 (2002); J. Catani, L. De Sarlo,

G. Barontini, F. Minardi, and M. Inguscio, Phys. Rev. A **77**, 011603(R) (2008); G. Thalhammer, G. Barontini, L. De Sarlo, J. Catani, F. Minardi, and M. Inguscio, Phys. Rev. Lett. **100**, 210402 (2008).

[37] S. B. Papp, J. M. Pino, and C. E. Wieman, Phys. Rev. Lett. **101**, 040402 (2008).

[38] C. A. Sackett, J. M. Gerton, M. Welling, and R. G. Hulet, Phys. Rev. Lett. **82**, 876 (1999); J. M. Gerton, D. Strekalov, I. Prodan, and R. G. Hulet, Nature **408**, 692 (2000); Elizabeth A. Donley, Neil R. Claussen, Simon L. Cornish, Jacob L. Roberts, Eric A. Cornell, and Carl E. Wieman, Nature (London) **412**, 295 (2001).

[39] D. S. Hall, M. R. Matthews, J. R. Ensher, C. E. Wieman, and E. A. Cornell, Phys. Rev. Lett. **81**, 1539 (1998); E. Timmermans, *ibid.* **81**, 5718 (1998); P. Ao and S. T. Chui, Phys. Rev. A **58**, 4836 (1998); R. A. Barankov, *ibid.* **66**, 013612 (2002).

[40] W. H. Press, S. A. Teukolsky, W. T. Vetterling, and B. P. Flannery, *Numerical Recipes. The Art of Scientific Computing* (Cambridge University Press, Cambridge, 1996).

[41] Samantha Hooley and Keith A. Benedict, Phys. Rev. A **75**, 033621 (2007).

[42] E. Timmermans, P. Tommasini, M. Hussein, and A. Kerman, Phys. Rep. **315**, 199 (1999); T. Kohler, K. Goral, and P. S. Julienne, Rev. Mod. Phys. **78**, 1311 (2006); C. Chin, R. Grimm, P. Julienne, and E. Tiesinga, e-print arXiv:0812.1496.